がん検診に有用な新しい腫瘍マーカーの開発
—膵癌の早期発見に向けた血清プロテオミクス—

分担研究者氏名：土田明彦
所属機関名：東京医科大学外科・消化器外科学
所属機関における職名：助教授

研究要旨

膵癌の早期発見に向けた血清プロテオミクスのために、東京医科大学医学倫理委員会の審査を経て、患者および健常者の血液を収集し、国立がんセンター研究所に搬入した。42名に研究への参加を依頼したところ、結果的に2名では血液採取を断念したが、残りの40名で血液採取を行った。現在までのところ、倫理的問題は生じておらず、また、搬送システムも問題なく稼動している。なお、液採取を行った40例の患者、健常者には、現在までのところ有害事象の報告はない。

A. 研究目的

膵管癌、膵管内乳頭粘液性癌などの膵臓悪性腫瘍は早期発見が困難であり、診断時には半数以上が遠隔転移を合併し手術不能である。また、手術可能な場合でも、多くの症例で術後2ー3年以内に再発し、化学療法や放射線療法などの補助療法もほとんど効果がなく、極めて予後不良である。近年、膵臓悪性腫瘍においても遺伝子レベルで種々の解析なされているが、治療成績の向上に結びつくような鍵となる遺伝子は見つかっていない。また、遺伝子レベルでの発現型では、しばしば最終的な機能とは結びつかず、ゲノム情報の最終的な表現型であるタンパク質全体（プロテオーム）を解析することが不可欠である。

本研究は、平成18年度厚生労働科学研究費補助金（第3次対がん総合戦略研究事業、主任研究者：国立がんセンター研究所　山田哲司部長）による多施設共同研究の一員として、膵がん、膵がん以外の疾患および健常者の血液を対象に、プロテオミクス技術を用いてタンパク質の発現解析およびこれらの相互関係を検討し、膵がんの早期発見に結びつく新しい腫瘍マーカーの開発あるいは新規抗癌剤開発への足がかりを追求することが目的である。この多施設共同研究の中で、我々が分担する研究項目は、患者および健常者の血清試料の採取、個人情報管理、臨床情報収得であり、倫理面への配慮を十分に行いながら、できる限りの血清試料を収集することにある。

B. 研究方法

東京医科大学病院で膵臓腫瘍の手術もしくは化学療法などの治療を予定している症例で、術前に別紙説明書を用いて、担当医より本研究に関しての説明を行い、同意の得られた症例のみを対象とした。また、対

照として、膵臓腫瘍を含めた癌を合併していない良性疾患患者、膵臓以外の臓器の腫瘍性疾患の患者、および病気を有していない健常者から同意を得て血液を採取した。できる限り速やかに、血液検体を遠心分離にかけて血球成分を分離し、分注後凍結保存する。匿名化した後、検体を凍結保存した状態で国立がんセンター研究所腫瘍プロテオミクスプロジェクトに搬入した。検体の搬入は、株式会社エスアールエル（本社：東京都立川市）に委託した。

本研究は国立がんセンター倫理委員会ならびに東京医科大学医学倫理委員会で審査され、いずれも承認された。研究説明、研究参加への同意の取得に関しては、以下の事項に留意し、倫理面への配慮を十分に行った。（以下、研究計画書より引用）

1) 本研究は、ヒトゲノムや遺伝子の解析を行うものではないが、厚生労働省、経済産業省が作成した「ヒトゲノム・遺伝子解析研究に関する倫理指針（平成13年3月29日）」や「ヘルシンキ宣言」の趣旨を踏まえて、人権の擁護、同意、危険性などへの配慮を十分に行うものとする。最も重要なことは、各人の権利の尊重によって確保される人間の尊厳のみならず、ヒトゲノムや遺伝子を含めた解析結果に関しても、種としての人間の尊厳を尊重することを基本姿勢として研究を行うこととする。
2) 試料提供者本人に十分理解が得られた時点で、本研究の目的と意義、研究協力の説明を口頭および文書をもって十分に行う。本人の意志が確認できない場合は、本研究の対象外とする。また、本研究の目的と意義、研究協力に同意しない場合でも何ら治療上の不利益を被らないこと、一旦同意をいただき検体を提供した後でも、提供者本人の希望で同意を撤回される場合には、データをすべて破棄し、研究対象から除外することなどを、提供者が理解しやすいよう、平易な言葉で説明する。本研究への参加および診療情報の研究利用への同意を得た後に署名を得る。
3) 提供された検体は、専用保存容器に入れ、当院および国立がんセンター研究所において超低温で保存しプロテオーム解析を行うが、この際、容器には提供者の氏名、年齢などの個人情報は一切記載せず、匿名化した検体識別番号のみを記載する。また、提供者の臨床データ（病名、血液データ、病理結果など）に関しても、匿名化して国立がんセンター研究所に提出し、厳重に管理・保存される。いかなる場合においても、個人情報は一切漏洩されないよう、厳重に保護・管理する。
4) 本研究により検体提供者が直接受ける利益はないが、本研究の成果が近い将来社会に還元され、予後不良な膵臓腫瘍の早期発見、治療の向上に役立つことが期待される。一方、このような科学的あるいは社会的利益が十分期待される研究であっても、提供者個人の人権の保障が最優先されることは言うまでもない。
5) 本研究では、血液13mlを採取するが、これによって、検体提供者の病状や治療に全く影響はない。万一、副作用などの健康被害が生じた場合には、当院の責任において迅速に対処することと

した。

6) 本研究では、血液検体を扱うため、検体提供者自身が被る危険性はほとんどないが、これらを取り扱う研究者はスタンダード・プレコーションを遵守して感染防御に務める。また、血液検体は、本研究のためにのみ用いられ、解析が終了した時点で、残った検体は、通常の処理方法で速やかに処理し、環境汚染等への危険性に関しても配慮する。

7) 本研究は、平成18年度厚生労働科学研究費補助金（第3次対がん総合戦略研究事業）による多施設共同研究であり、研究分担の補助金が支給される。その他、企業などからの資金はない。なお、提供者本人に関しては、研究参加に対する対価は一切支払われない。

8) 本研究は、平成18年度厚生労働科学研究費補助金（第3次対がん総合戦略研究事業）による多施設共同研究として実施されるため、研究全体の社会的、倫理的問題については、国立がんセンターの倫理審査委員会で、また、当院での実施にあたっては、東京医科大学医学倫理委員会で厳正な審査を行ない、両者の認可を得て実施することとする。提供者本人あるいは提供者の家族などから社会的、倫理的問題に対して疑義照会や苦情があった場合には、研究総括責任者あるいは研究代表者が誠実に対応する。

C. 研究結果

国立がんセンター倫理審査委員会および東京医科大学医学倫理委員会の承認を得た後、42名の患者および健常者に本研究への参加を依頼した。その結果、平成19年2月25日現在で40名より血液を採取して型どおりの処理を行った。疾患の内訳は、膵臓癌：10例、膵臓良性疾患：3例、胃癌：9例、胆道癌：1例、大腸癌：10例、健常者7例であった。血液検体は、匿名化した後に、病院内の中央検査部に常駐する株式会社エスアールエルの職員に渡し、同社の集配システムに載せて国立がんセンター研究所に搬入したが、この過程での問題はまったく生じなかった。また、倫理面での配慮に関しても、すべての血液検体で匿名化が行われ、個人情報が漏洩するような事態は生じなかった。

血液採取が不能であった2名に関しては、1名は本研究への参加の同意が得られ血液採取を試みたが、末梢静脈が細いために途中で血液採取を断念した。残りの1名は、本研究の趣旨を説明したが、当初より参加の同意が得られなかった。

D. 考察

膵癌の血液診断として、CEA、CA19-9などの腫瘍マーカーの測定が行われているが、比較的早期のTS1膵癌の陽性率は、CEA約30%、CA19-9約50%とけっして高くはない。また、膵癌では膵管狭窄や閉塞によって、アミラーゼ、リパーゼ、エラスターゼ1などの膵酵素が上昇するが、長期間は持続せず、TS1膵癌における陽性率は腫瘍マーカーと同程度に低い。また、TS1膵癌では自覚症状に乏しく、これらの事実が膵癌の早期発見を妨げる要因となってい

る。

近年、プロテオーム技術を用いて血液中に含まれる低分子蛋白質を網羅的にプロファイルすることが可能となってきている。なかでも、SELDI-TOF-MSという方法を用いて血液含有ペプチドを網羅的に解析する方法が注目を集めている。本研究では、この方法を用いて、個々の血清ペプチドの発現に注目するのではなく、対照群との比較によって、それぞれの病態に特徴的なパターンをコンピューターで解析する診断法を開発し、膵癌の早期発見の新しいマーカーとしての有用性を検討することを目的とした。既に、国立がんセンター中央病院と我々の施設の症例を対象とした基礎研究において、4つのペプチドの発現をみることによって、90%以上の確率で膵癌患者を識別できることが立証されている（Honda et al: Cancer Res 65:10613-10622, 2005）。この多施設共同研究では、さらに症例を重ねることによって、この方法の有用性を再確認するとともに、近い将来の臨床応用に向けて、血液検体の搬送方法や短期間での結果報告など、システム全体の構築を目指しているものである。現在までのところ、研究結果に記載したように、倫理面での問題は発生しておらず、また、搬送システムにおいても問題は生じておらず、きわめて順調に経過している。今後、さらに症例を収集し、本研究に寄与することが望まれる。

E. 結論

膵癌の早期発見に向けた血清プロテオミクスのために、倫理委員会の審査を経て、患者および健常者の血液を収集し、国立がんセンター研究所に搬入した。現在までのところ、倫理的問題は生じておらず、また、搬送システムも問題なく稼動している。

F. 健康危険情報

血液採取を行った40例の患者、健常者には、現在までのところ有害事象の報告はない。

G. 研究発表

1．論文発表

1) Osaka Y, Takagi Y, Hoshino S, Tachibana S, Tsuchida A, Aoki T: Combination chemotherapy with docetaxel and nedaplatin for recurrent esophageal cancer in an outpatient setting. Dis Esophagus 2006;19(6):473-476

2) Katsumata K, Sumi T, Mori Y, Hisada M, Tsuchida A, Aoki T: Detection and evaluation of epithelial cells in the blood of colon cancer patients using RT-PCR. Int J Clin Oncol 2006;11(5):385-399.

3) 粕谷和彦、土田明彦、青木達哉：抗体エンジニアリング．東京医科大学雑誌 2006;64(3):222-228.

4) 土田明彦、長江逸郎、齋藤　準、池田隆久、田辺好英、高橋総司、青木達哉、糸井隆夫：膵・胆管合流異常における胆道発癌の予防．臨床消化器内科 2006;21(6):705-709.

5) 須藤日出男、高木　融、片柳　創、星野澄人、須田　健、日比康太、伊藤一

成、土田明彦、青木達哉：胃がん骨転移．癌と化学療法
2006;33(8):1058-1060.

2．学会発表

1）Nagakawa Y, Tsuchida A, Ozawa T, Kasuya K, Saito H, Ikeda T, Aoki T: Effectiveness of intraoperative frozen section for diagnosis of unsuspected gallbladder cancer during laparoscopic surgery. 16th China-Japan Joint Congress for Gastroenterological Surgery

2）Aoki To, Suzuki Y, Sumi T, Takagi M, Yasuda Y, Yoneda K, Ogata T, Nomura T, Tsuchida A, Aoki T: Our technique of pancreaticogastrostomy following pancreaticoduodenectomy. 16th China-Japan Joint Congress for Gastroenterological Surgery

3）榎本正統、土田明彦、横山智央、鴇田博美、宮澤啓介、青木達哉：胆管細胞癌細胞株におけるVitamin K2の抗腫瘍効果に関する検討。第61回日本消化器外科学会総会

4）永川裕一、土田明彦、小澤 隆、粕谷和彦、斎藤 準、池田隆久、遠藤光史、冨岡英則、青木達哉：尾側膵切除における膵切離方法と膵液瘻発生の検討。第61回日本消化器外科学会総会

5）逢坂由昭、高木 融、星野澄人、立花慎吾、林田康治、土田明彦、青木達哉、本田一文、山田哲司：血中プロテオーム解析による食道癌術前化学放射線療法の効果予測。日本ヒトプロテオーム機構第4回大会、第2回日本臨床プロテオーム研究会

6）日比康太、岩屋啓一、土田明彦、青木達哉、向井 清：通常型膵管癌と膵管内乳頭粘液性腫瘍（IPMNs）との浸潤転移との関係。第44回日本癌治療学会総会

7）永川裕一、土田明彦、粕谷和彦、小澤 隆、斎藤 準、池田隆久、青木達哉：Gemcitabineによる膵癌術後補助化学療法の安全性と有効性。第68回日本臨床外科学会総会

H．知的財産権の出願・登録状況

現在のところ、知的財産権の出願・登録はない。

厚生労働科学研究補助金（第３次対がん総合戦略研究事業）
分担研究報告書

がん検診に有用な新しい腫瘍マーカーの開発

分担研究者　氏名　斎藤　豊　所属　内視鏡部　職名　医員

研究要旨
精密検診の前スクリーニングに応用できる新規腫瘍マーカーを開発することを最終目標とする。早期胃癌・早期大腸がんおよび健常者より血液検体と臨床情報を収集し、低流速液体クロマトグラフィーや質量分析などのプロテオミクスの先端技術を駆使し、血漿・血清中に存在するタンパク質、ペプチドの大規模な定量解析を行い、診断に有用な分子を同定し、臨床応用可能性を検討する。

A．研究目的

がん検診無症状の段階でがんを発見し早期に治療を開始することが有効ながん対策法の一つと考えられる。被験者の負担が少なく非侵襲的に得られる血液を検体に用い、精密検診を行うべく症例を効率良く絞るプレスクリーニングに使用でき新規腫瘍マーカーを開発することを目的とする。

B．研究方法

平成18年度10月より内視鏡外来に来院した①早期胃癌②早期大腸癌③健常者（検診目的の患者）から血液検体および臨床情報を収集する。

（倫理面への配慮）

試験実施に際しては、倫理委員会の承認を得て、またすべての患者から事前に同意を得た。

C．研究結果

平成18年10月から平成19年度3月まで内視鏡外来を受診した早期胃癌患者、早期大腸癌患者、健常者から採血の同意を得た。

D．考察

現在、早期胃癌および早期大腸癌を診断するためには内視鏡検査が不可欠であるが、患者苦痛や内視鏡医のマンパワー不足から、簡便で多数の患者を一度にスクリーニングできるシステムが望まれている。

E．結論

今回は、早期胃癌患者、早期大腸癌患者、健常者からの採血の同意が得られたのみで血液バイオマーカーによるがん検診の可能性については不明である。今後、この検討から、内視鏡治療で完治が望まれる早期胃癌・大腸癌が採血のみで診断できるようなバイオマーカーが同定されれば、臨床上非常に有用である。

F．健康危険情報

特になし。

G．研究発表

1.論文発表

1. Uraoka T, Saito Y, Matsuda T, Ikehara H, Gotoda T, Saito D, Fujii T. Endoscopic indications for endoscopic mucosal resection of laterally spreading tumours in the colorectum.. Gut. 2006; 55(11):1592-7.

2. Saito Y, Uraoka T, Matsuda T, Emura F, Ikehara H, Mashimo Y, et al. A pilot study to assess safety and efficacy of carbon dioxide insufflation during colorectal endoscopic submucosal dissection under conscious sedation. Gastrointest Endosc 2007;65(3):537-42.

3. Saito Y, Uraoka T, Matsuda T, et al. Endoscopic treatment of large superficial colorectal tumors: A cases series of 200 endoscopic submucosal dissections (with video). Gastrointest Endosc 2007 *in press.*

2.学会発表

1. Yutaka Saito, et al. Oral Presentation. Is en-bloc resection of large colorectal tumors feasible? Results of 120 cases of endoscopicsubmucosal dissection. ASGE 10th Annual VideoForum at DDW Held in Petree Hall of the Los Angeles Convention Center on Monday, May 22, 2006, from 8:00 am to 12:00 pm.

2. Yutaka Saito, et al. A PILOT TRIAL STUDY TO ASSESS SAFETY AND EFFICACY OF CARBON DIOXIDE INSUFFLATION DURING COLORECTAL ENDOSCOPIC SUBMUCOSAL DISSECTION. Poster presentation

during Digestive Disease Week, to be held at the Los Angeles Convention Center in Los Angeles, California, May 20-25, 2006.
3. Yutaka Saito. Endoscopic diagnosis and treatment for early colorectal cancers. ESSE-1st European Congress for Surgical Endoscopy, June 1, 2006, Verona, Italy
4. Yutaka Saito. Endoscopic diagnosis and treatment for early gastric and colonic cancers. National Congress 'Frontiers in Endoscopic Therapy and Surgery', June 7, 2006, Porto, Portugal
5. Yutaka Saito, et al. Oral video presentation. ENDOSCOPIC SUBMUCOSAL DISSECTION FOR RECURRENT COLORECTAL TUMORS. The 14 th United European Gastroenterology Week (UEGW), October 23, 2006, Berlin, German
6. Yutaka Saito, et al. Oral video presentation. ENDOSCOPIC SUBMUCOSAL DISSECTION FOR RECURRENT COLORECTAL TUMORS. The 14 th United European Gastroenterology Week (UEGW), October 23, 2006, Berlin, German
7. Yutaka Saito, et al. Narrow Band Imaging diagnosis for early colorectal cancer. 6th congress of gastroenterology of south east Asian nations, 12th Vnage annual scientific meeting. Hanoi October, 19-21/2006. International Convention Center
8. Yutaka Saito. Endoscopic diagnosis and treatment for early esophageal and colorectal cancer. Cancer 2006, Bogota, Colombia, November 9, 2006.
9. Yutaka Saito. Endoscopic diagnosis and treatment for early colorectal cancer. ELBOSQUE University, Bogota, Colombia, November 8, 2006.
10. Yutaka Saito. Endoscopic diagnosis and treatment for early esophageal and colorectal cancer. ELBOSQUE University, Bogota, Colombia, November 8, 2006.
11. Yutaka Saito, et al. EMR and ESD for colorectal tumors. ISDS (International Colorectal Disease Symposium) 2007 in Hong Kong. Jan. 25-27, 2007 Hong Kong Convention & Exhibition Centre, Hong Kong SAR, China.
12. Yutaka Saito, et al. 9th International Symposium: Diagnostic and therapeutic Endoscopy 2nd and 3rd of February 2007 in Düsseldorf
Live demonstration of EMR and ESD for colon LST and rectal LST
Lecture: Piecemeal and en-bloc resection of colorectal lesions: when and how?

H. 知的財産権の出願・登録状況（予定を含む）
1. 特許取得
なし
2. 実用新案登録
なし
3. その他
なし

研究成果の刊行に関する一覧表

雑誌

発表者氏名	論文タイトル名	発表誌名	巻号	ページ	出版年
Hara T, Honda K, Shitashige M, Ono M, Matsuyama H, Naito K, Hirohashi S, Yamada	Mass spectrometry analysis of the native protein complex containing actinin-4 in prostate cancer cells.	Mol Cell Proteomics.			in press
Kikuchi S, Honda K, Handa Y, Kato H, Yamashita K, Umaki T, Ono M, Tsuchida A, Aoki T, Hirhashi S, Yamada T.	Serum Albumin-Associated Peptides of in Patients with Uterine Endometrial Cancer.	Cancer Sci.			in press
Shitashige M, Naishiro Y, Idogawa M, Honda K, Ono M, Hirohashi S, Yamada T.	Involvement of Splicing Factor-1 in β-Catenin/T Cell Factor-4-mediated Gene Transactivation and Pre-mRNA Splicing.	Gastro-enterology	132	1039	2007
Kakisaka T, Kondo T, Okano T, Fujii K, Honda K, Endo M, Tsuchida A, Aoki T, Itoi T, Moriyasu F, Yamada T, Kato H, Nishimura T, Todo S, Hirohashi S.	Plasma proteomics of pancreatic cancer patients by multi-dimensional liquid chromatography and two-dimensional difference gel electrophoresis (2D-DIGE): Up-regulation of leucine-rich alpha-2-glycoprotein in pancreatic cancer.	J Chromatogr B Analyt Technol Biomed Life			in press
Idogawa M, Masutani M, Shitashige M, Honda K, Tokino T, Shinomura Y, Imai K, Hirohashi S, Yamada T.	Ku70 and poly(ADP-ribose) polymerase-1 competitively regulate beta-catenin and T-cell factor-4-mediated gene transactivation: Possible linkage of DNA damage recognition and Wnt signaling.	Cancer Res.	67	911	2007
Ono M, Shitashige M, Honda K, Isobe T, Kuwabara H, Matsuzuki H, Hirohashi S, Yamada T.	Label-free quantitative proteomics using large peptide data sets generated by nanoflow liquid chromatography and mass spectrometry.	Mol Cell Proteomics	5	1338	2006
本田一文 逢坂由昭、土田明彦、青木達哉、山田哲司	放射線感受性 －血清ペプチドプロファイルを用いた食道がん術前化学放射線療法奏効性予測の可能性	別冊医学のあゆみ	341		2006
下重美紀、本田一文、山田哲司	血液試料の最適な調整法と解析	バイオテクノロジージャーナル	3-4	148	2006
本田一文、山田哲司	腫瘍マーカーと包括的プロテオーム解析：ペプチドの包括的プロファイリングによる非侵襲的腫瘍マーカー開発	分子呼吸器病	10	133	2006
本田一文、尾野雅哉、下重美紀、山田哲司	'膵癌'早期発見の新技術	日本臨床	64	1745	2006
本田一文、山田哲司	ゲノム・プロテオーム情報を利用した薬剤感受性・副作用予測	臨床と研究	83	1270	2006
山田哲司、本田一文	プロテオミクス解析による膵臓がんの血漿マーカーの開発	ファルマシア	43	32	2007
尾野雅哉、本田一文、山田哲司	バイオテクノロジーのがん検診への応用とその将来性	公衆衛生	71	100	2007
尾野雅哉、本田一文、山田哲司	腫瘍マーカー	クリニカル プラクティス	26	235	2007
本田一文、尾野雅哉、山田哲司	血漿・血清がん診断法、新たな検診方法はあるのか。－血漿ペプチドプロファイルによる難治がん患者検出の可能性	呼吸器コモンディジィーズ 肺がんのすべて		49	2007
下重美紀、本田一文、尾野雅哉、山田哲司	プロテオミクスの臨床応用への期待	Annual Review 呼吸器		208	2007

発表者氏名	論文タイトル名	発表誌名	巻号	ページ	出版年
本田一文、尾野雅哉、下重美紀、山田哲司	質量分析をもちいた血清・血漿プロテオーム解析によるがん診断マーカー開	細胞工学			印刷中
本田一文、山田哲司	がん転移・浸潤に対するアクチン結合たんぱく質アクチニン-4の生物学的機能	生化学			印刷中
小泉大、佐田尚宏、永井秀雄	膵癌の腫瘍マーカー	Surgery Frontier			印刷中
井岡達也、田中幸子	膵癌	総合臨牀	55	1086	2006
井岡達也、中泉明彦、田中幸子、山崎秀哉、西山謹	Gemcitabine併用化学放射線療法	日本臨牀	64	248	2006
中泉明彦、石田哲士、高倉玲奈、高野保名、井岡達也、沖尾美穂、鈴木玲子、福田順子、上原宏之、津熊秀明、田中幸子	検診による膵癌早期診断	臨牀消化器内科	21	1725	2006
中泉明彦、石田哲士、高倉玲奈、高野保名、井岡達也、沖尾美穂、鈴木玲子、福田順子、上原宏之、津熊秀明、田中幸子	膵癌検診システムにおける高危険群	胆と膵	27	131	2006
Okusaka T, Ishii H, Funakoshi A, Yamao K, Ohkawa S, Saito S, Saito H, Tsuyuguchi T.	Phase II study of single-agent gemacitabine in patients with advanced biliary tract cancer.	Cancer Chemother Pharmacol	57	647	2006
Okusaka T, Yamada T, Maekawa M.	Serum tumor markers for pancreatic cancer: The dawn of new era?	Journal of the Pancreas	7	332	2006
Okusaka T, Ishii H, Funakoshi A, Ueno H, Furuse J, Sumii T.	A phase I/II study of combination chemotherapy with gemcitabine and 5-fluorouracil for advanced pancreatic cancer.	Jpn J Clin Oncol.	36	557	2006
Ueno H, Sato T, Yamamoto S, Tanaka K, Ohkawa S, Takagi H, Yokosuka O, Furuse J, Ishii H, Sawaki A, Kasugai H, Osaki Y, Fujiyama S, Sato K, Wakabayashi K, Okusaka T.	Randomized, double-blind, placebo-control trial of orally administered bovine lactoferrin in patients with chronic hepatitis C.	Cancer Sci.	97	1105	2006
Takayasu K, Muramatsu Y, Mizuguchi Y, Moriyama N, Okusaka T.	Multiple on-tumors arterioportal shunts due to chronic liver disease mimicking hepatocellular carcinoma: outcomes and the associated elevation of alpha-fetoprotein.	J Gastroenterol Hepatol.	21	288	2006
Takayasu K, Muramatsu Y, Mizuguchi Y, Okusaka T, Shimada K, Takayama T, Sakamoto M.	CT Evaluation of the Progression of Hypoattenuating Nodular Lesions in Virus-Related Chronic Liver Disease.	AJR.	187	454	2006
Furuse J, Okusaka T, Funakoshi A, Yamoo K, Nagase M, Ishii H, Nakachi K, Ueno H, Ikeda M, Morizane C, Horikawa Y, Mizuno N.	Early phase II study of uracil-tegafur plus doxorubicin in patients with unresectable advanced biliary tract cancer.	Jpn J Clin Oncol.	36	552	2006
Kondo S, Okusaka T, Ueno H, Ikeda M, Morizane C.	Spontaneous regression of hepatocellular carcinoma.	Int J Clin Oncol.	11	407	2006

発表者氏名	論文タイトル名	発表誌名	巻号	ページ	出版年
Ito Y, Okusaka T, Kagami Y, Ueno H, Ikeda M, Sumi M, Imai A, Fujimoto N, Ikeda H.	Evaluation of acute intestinal toxicity in relation to the volume of irradiated small bowel in patients treated with concurrent weekly gemcitabine and radiotherapy for locally advanced pancreatic cancer.	Anticancer Res.	26	3755	2006
Ueno H, Okusaka T, Funakoshi A, Ishii H, Yamao K, Ishikawa O, Ohkawa S, Saitoh S.	A phase II study of weekly irinotecan as first-line therapy for patients with metastatic pancreatic cancer.	Cancer Chemother Pharmacol.	59	447	2007
Sugiyama E, Kaniwa N, Kim SR, Kikura-Hanajiri R, Hasegawa R, Maekawa K, Saito Y, Ozawa S, Sawada J, Kamatani N, Furuse J, Ishi H, Yoshida T, Ueno H, Okusaka T, Saijo N.	Pharmacokinetics of gemcitabine in Japanese cancer patients: The impact of a cytidine deaminase polymorphism.	J Clin Oncol.	25	32	2007
Okusaka T, Funakoshi A, Furuse J, Boku N, Yamao K, Ohkawa S, Saito H.	A late phase II study of S-1 for metastatic pancreatic cancer.	Cancer			in press
Ueno H, Okusaka T, Ikeda M, Morizane C.	Phase II study of combination chemotherapy with gemcitabine and cisplatin for patients with metastatic	Jpn J Clin Oncol			in press
Takayasu K, Mizuguchi Y, Muramatsu Y, Okusaka T, Takayama T, Sakamoto M.	Natural outcome of hypovascular nodular lesion of chronic liver disease studied by follow-up CT; analysis of factors affecting malignant trasformation.	Radiology			in press
奥坂拓志、上野秀樹、池田公史、森実千種	膵癌診断の進歩－内科の立場から	消化器病学会雑誌	103	391	2006
奥坂拓志、上野秀樹、池田公史、森実千種	膵癌　TS-1単剤治療について	癌と化学療法	33	207	2006
奥坂拓志	ゲムシタビンとS-1の併用療法	薬事日報	10266	4	2006
奥坂拓志	胆道系がん	新臨床腫瘍学		451	2006
上野秀樹、奥坂拓志	6.切除不能膵癌の治療 (3)化学療法	コンセンサス癌治療	5	40	2006
上野秀樹、奥坂拓志	進行膵癌の予後改善を目指す治療戦略　特集Ⅰ 進行消化器癌の予後改善を目指す治療戦略	消化器科	42	146	2006
上野秀樹、奥坂拓志	切除不能膵がんの化学療法の現状と今後の課題	血液・腫瘍科	53	436	2006
池田公史、名嶋弥菜、森実千種、上野秀樹、奥坂拓志	胆道癌症例と緩和医療. B. 胆道癌. Ⅸ. 胆道癌治療におけるQOL. 膵癌・胆道癌の診断と治療－最新の研究動向	日本臨床	64	556	2006
池田公史、奥坂拓志	53.肝細胞癌. Common Disease インストラクション・マニュアル－患者に何をどう説明するか－	Medicina	43	203	2006
池田公史、奥坂拓志	腫瘍マーカーの限界は. 特集 肝細胞がん患者にどう対応するか. 2.肝細胞がんの診断―見落としを防ぐコツ―	臨床プラクティス	2	350	2006
森実千種、奥坂拓志、上野秀樹、池田公史	5－FU系. B. 胆道癌. Ⅶ. 胆道癌の治療. 4. 進行・再発胆道癌の治療. 膵癌・胆道癌の診断と治療－最新の研究動向	日本臨床	64	529	2006
名嶋弥菜、奥坂拓志	腫瘍マーカーによる診断. B. 胆道癌. Ⅲ. 胆道癌の病理. 膵癌・胆道癌の診断と治療－最新の研究動向－	日本臨床	64	419	2006
池田公史、森実千種、上野秀樹、奥坂拓志	肝外転移を有するFMP療法の治療成績と効果. 特集Ⅱ「進行肝癌の治療最	消化器科	43	234	2006

発表者氏名	論文タイトル名	発表誌名	巻号	ページ	出版年
Osaka Y, Takagi Y, Hoshino S, Tachibana S, Tsuchida A, Aoki T.	Combination chemotherapy with docetaxel and nedaplatin for recurrent esophageal cancer in an outpatient setting.	Dis Esophagus	19	473	2006
Katsumata K, Sumi T, Mori Y, Hisada M, Tsuchida A, Aoki T.	Detection and evaluation of epithelial cells in the blood of colon cancer patients using RT-PCR.	Int J Clin Oncol.	11	385	2006
粕谷和彦、土田明彦、青木達哉	抗体エンジニアリング	東京医科大学雑誌	64	222	2006
土田明彦、長江逸郎、齋藤準、池田隆久、田辺好英、高橋総司、青木達哉、糸井隆夫	膵・胆管合流異常における胆道発癌の予防	臨床消化器内科	21	705	2006
須藤日出男、高木　融、片柳創、星野澄人、須田　健、日比康太、伊藤一成、土田明彦、青木達哉	胃がん骨転移	癌と化学療法	33	1058	2006
Isomura K, Kono S, Moore MA, Toyomura K, Nagano J, Mizoue T, Mibu R, Tanaka M, Kakeji Y, Maehara Y, Ikejiri K, Futami K, Yasunami Y, Maekawa T, Takenaka K, Ichimiya H, Imaizumi N.	Physical activity and colorectal cancer: The Fukuoka colorectal cancer study.	Cancer Sci.	97	1099	2006
Iwai T, Tomita Y, Okano S, Shimizu I, Yasunami Y, Kajiwara T, Yoshikai Y, Taniguchi M, Nomoto K, Yasui H.	Regulatory roles of NKT cells in the induction and maintenance of cyclophosphamide-induced tolerance.	J Immunol.	177	8400	2006
Kajiwara T, Tomita Y, Okano S, Iwai T, Yasunami Y, Yoshikai Y, Nomoto K, Tominaga R, Yasui H.	Effects of cyclosporin A on the activation of NKT cells induced by alpha-galactosylceramide.	Transplantation			in press
Yokoo H, Kondo T, Okano T, Nakanishi K, Sakamoto M, Kosuge T, Todo S, Hirohashi S.	Protein expression associated with early intrahepatic recurrence of hepatocellular carcinoma after curative surgery.	Cancer Sci.			in press
Okano T, Kondo T, Fujii K, Nishimura T, Takano T, Ohe Y, Tsuta K, Matsuno Y, Gemma A, Kato H, Kudoh S, Hirohashi S.	Proteomic signature corresponding to the response to gefitinib (Iressa, ZD1839), an epidermal growth factor receptor (EGFR) tyrosine kinase inhibitor, in lung adenocarcinoma.	Clin Cancer Res.	13	799	2006
Kondo T and Hirohashi S.	Application of highly sensitive fluorescent dyes (CyDye DIGE Fluor Saturation Dyes) to laser microdissection and two-dimensional difference gel electrophoresis (2D-DIGE) for cancer proteomics.	Nature Protocols	1	2940	2007
Hatakeyama H, Kondo T, Fujii K, Nakanishi Y, Kato H, Fukuda S, Hirohashi S.	Proteomic study identified protein clusters associated with carcinogenesis, histological differentiation and nodal metastasis of esophageal cancer.	Proteomics	6	6300	2006
Fujii K, Kondo T, Yamada M, Iwatsuki K, Hirohashi S.	Toward a comprehensive quantitative proteome database: protein expression map of lymphoid neoplasms by 2-D DIGE and MS.		6	4856	2006

発表者氏名	論文タイトル名	発表誌名	巻号	ページ	出版年
Suehara Y, Kondo T, Fujii K, Hasegawa T, Kawai A, Seki K, Beppu Y, Nishimura T, Kurosawa H, Hirohashi S.	Proteomic signatures corresponding to histological classification and grading of soft-tissue sarcomas.	Proteomics	6	4402	2006
Okano T, Kondo T, Kakisaka T, Fujii K, Yamada M, Kato H, Nishimura T, Gemma A, Kudoh S, Hirohashi S.	Plasma proteomics of lung cancer by a linkage of multi-dimensional liquid chromatography and two-dimensional difference gel electrophoresis.	Proteomics	6	3938	2006
近藤格	疾患プロテオミクスと蛍光ディファレンシャル二次元電気泳動	生物物理化学	50	155	2006
近藤格	二次元電気泳動法と質量分析のための組織試料の調製法	バイオテクノロジージャーナル	6	153	2006
近藤格、廣橋説雄	がんのプロテオミクス	新臨床腫瘍学		83	2006
Uraoka T, Saito Y, Matsuda T, Ikehara H, Gotoda T, Saito D, Fujii T.	Endoscopic indications for endoscopic mucosal resection of laterally spreading tumours in the colorectum.	Gut.	55	1592	2006
Saito Y, Uraoka T, Matsuda T, Emura F, Ikehara H, Mashimo Y, et al.	A pilot study to assess safety and efficacy of carbon dioxide insufflation during colorectal endoscopic submucosal dissection under conscious sedation.	Gastrointest Endosc.	65	537	2007
Saito Y, Uraoka T, Matsuda T, et al.	Endoscopic treatment of large superficial colorectal tumors: A cases series of 200 endoscopic submucosal dissections (with video).	Gastrointest Endosc.			in press

Label-free Quantitative Proteomics Using Large Peptide Data Sets Generated by Nanoflow Liquid Chromatography and Mass Spectrometry*

Masaya Ono‡, Miki Shitashige‡, Kazufumi Honda‡, Tomohiro Isobe§, Hideya Kuwabara§, Hirotaka Matsuzuki§, Setsuo Hirohashi‡, and Tesshi Yamada‡¶

We developed an integrated platform consisting of machinery and software modules that can apply vast amounts of data generated by nanoflow LC-MS to differential protein expression analyses. Unlabeled protein samples were completely digested with modified trypsin and separated by low speed (200 nl/min) one-dimensional HPLC. Mass spectra were obtained every 1 s by using the survey mode of a hybrid Q-TOF mass spectrometer and displayed in a two-dimensional plane with *m/z* values along the *x* axis, and retention time was displayed along the *y* axis. The time jitter of nano-LC was adjusted using newly developed software based on a dynamic programming algorithm. The comprehensiveness (60,000–160,000 peaks above the predetermined threshold detectable in 60-μg cell protein samples), reproducibility (average coefficient of variance of 0.35–0.39 and correlation coefficient of over 0.92 between duplicates), and accurate quantification with a wide dynamic range (over 10^3) of our platform warrant its application to various types of experimental and translational proteomics. *Molecular & Cellular Proteomics 5:1338–1347, 2006.*

Because of the large diversity in the physical and chemical characteristics of proteins no single platform capable of analyzing the entire protein content (or proteome) of complex biological specimens, such as tissue extracts, cell lysates, blood plasma/serum, and other body fluids, is currently available. For example, two-dimensional gel electrophoresis, a widely used proteome platform, is inadequate for analysis of high molecular weight, hydrophobic, or highly acidic/basic proteins (1, 2). So-called "shotgun" proteomics is an emerging concept that has been developed to cope with this problem (3, 4). Protein sample is enzymatically digested into a large array of small peptide fragments (or peptide array) (5). The protein composition of immunoprecipitates, organelles, cultured cells, and clinical samples have been thoroughly identified by the combination of multidimensional LC and MS/MS (3, 6–9).

Although each peptide fragment of peptide arrays represents the relative abundance of its source protein, MS/MS may not be powerful enough as a means of quantification. Because selection of precursor ions for MS/MS may not be constant from experiment to experiment, low abundance proteins can be easily overlooked (10). Several types of *in vivo* metabolic and *in vitro* chemical and enzymatic isotope labeling methods including ICAT, SILAC (stable isotope labeling by amino acids in cell culture), and iTRAQ (isobaric tagging for relative and absolute quantitation) have been developed to add a quantitative dimension to MS/MS (11–13). However, *in vivo* labeling cannot be used for clinical samples, and the efficiency of labeling cannot be matched completely in a large number of samples.

Several attempts have made to quantify peptides generated from unlabeled protein samples by LC-MS instead of LC-MS/MS (5, 14, 15) because there is a linear correlation between MS signal intensities and the relative quantity of peptides (14, 16). However, comparison of different LC-MS data sets is still challenging because of the unsteady flow of LC (17). *Li* et al. (10) recently tried to overcome this problem by developing a new software suit, namely SpecArray, that is capable of comparing multiple LC-MS data by aligning LC flows. They purified *N*-glycosylated proteins prior to LC-MS to reduce the sample complexity to a level capable of being managed by their software (5).

The dynamic programming algorithm has been used for comparing large, similar DNA sequences with high accuracy and speed (18); it may be applicable to the alignment of large LC-MS data sets obtained at slightly different LC flows. We also developed a series of software modules suitable for the detection, visualization, quantification, and comparison of LC-MS data generated from unlabeled and unpurified protein samples. The refinement of the nanoflow HPLC system was also necessary to achieve high sensitivity and reproducibility. The high mass accuracy and constancy of Q-TOF MS instru-

From the ‡Chemotherapy Division and Cancer Proteomics Project, National Cancer Center Research Institute, Tokyo 104-0045 and §BioBusiness Group, Mitsui Knowledge Industry, Tokyo 164-8555, Japan

Received, November 18, 2005, and in revised form, March 13, 2006
Published, MCP Papers in Press, March 21, 2006, DOI 10.1074/mcp.T500039-MCP200

ments can eliminate mismatching by narrowing the mass tolerance (16). We integrated all of the machinery and software elements into a new proteomic platform called 2-dimensional image-converted analysis of liquid chromatography and mass spectrometry (2DICAL).[1]

EXPERIMENTAL PROCEDURES

Cell Culture and Sample Preparation

The colorectal cancer cell clone capable of inducing an actin-binding protein, actinin-4, under the strict control of the tetracycline-regulatory promoter system (DLD1 Tet-Off ACTN4) has been described previously (19). Induction of actinin-4 has been found to significantly increase cell motility and cause lymph node metastasis in experimental animals. Pancreatic cancer cell lines BxPC3 and Capan-1 have been described previously (20). BxPC3 is a cell line with high cell motility, and Capan-1 is a cell line with low cell motility. Cell lysates were prepared with buffer containing 0.01 M Tris-HCl, pH 7.4, 0.14 M NaCl, 1% Triton X-100, and a protease inhibitor mixture (Sigma). A blood specimen was collected from a healthy volunteer. Plasma was obtained by centrifugation at 3000 rpm for 30 min and cryopreserved at −80 °C until analyzed (21).

To each 100 μl of cell lysate (3 mg/ml) or 5 μl of plasma, 900 μl of cold acetone (−20 °C) was added, and the samples were maintained at −20 °C for 20 min. After centrifugation at 17,400 × *g* for 10 min, the pellet was dissolved in 250 μl of distilled water and reprecipitated with cold acetone. Then 10 μl of 5 M urea, 2.5 μl of 1 M NH_4HCO_3, and 3.3 μg of sequencing grade modified trypsin (Promega, Madison, WI) were added, and a final volume of 50 μl was achieved by adding distilled water. After digesting at 37 °C for 20 h, peptides were extracted with 50 μl of acetonitrile, dried with a SpeedVac concentrator (Thermo Electron, Holbrook, NY), and then dissolved in 50 μl of 0.1% formic acid.

LC-MS

The splitless nanoflow HPLC system equipped with reversed-phase columns (inner diameter, 0.15 mm; 50 mm long) was constructed in collaboration with KYA (Tokyo, Japan). The columns were packed with the finest grade spherical silica gel chemically bonded with octadecyl groups. The average particle size of the material was 3 μm, and pore size was 120 Å. A 10-μl protein sample was separated at a speed of 200 nl/min with a linear gradient from 0–80% acetonitrile, 0.1% formic acid for 60 min. Mass spectra were acquired with an ESI-Q-TOF mass spectrometer (QTOF Ultima, Waters) in the 250–1600 *m/z* range every second for 60 min.

Peak Detection

The peak detection software was a modification of MassNavigator™ (Mitsui Knowledge Industry, Tokyo, Japan), and performs the following steps (Steps 1–3).

Step 1—After base-line compensation for every spectrum, signals with a signal to noise ratio greater than 2 are selected.

Step 2—Mass signals are fitted to the isotope distribution model below, and the monoisotopic molecular weight and ion charge number are calculated (22, 23).

$$T(m') \equiv h \cdot \sum_{i=0}^{\infty} p_m^{\mathrm{iso}}(i) \cdot e^{\frac{((m'-m-i)/c)^2}{2\sigma^2}} \qquad \text{(Eq. 1)}$$

where T is the isotope distribution model with the function m', m' is molecular weight measured by MS, h is intensity, m is monoisotopic molecular weight, c is ion charge number, and σ is the width of the Gaussian distribution, which represents the distribution of each peak.

$p_m^{\mathrm{iso}}(i)$ is the distribution of the isotope ratio and is approximated by a Poisson distribution. Thus

$$p_m^{\mathrm{iso}}(i) \equiv \frac{e^{-M} \cdot M^i}{i!} \qquad \text{(Eq. 2)}$$

where

$$M(m) = 0.000594 \times m - 0.0309. \qquad \text{(Eq. 3)}$$

The intensity of isotopic mass was added to the monoisotopic molecular weight, and the summed monoisotopic intensity was the represented value in the next step.

Step 3—When the signals had the same ion charge number within 0.2 *m/z* in the consecutive spectrum before or after, the signals were grouped. The peak intensity was defined as the sum of ion intensity of the grouped signals, *m/z* was defined as the monoisotopic molecular weight, and retention time (RT) was defined as the time corresponding to the central gravity of the ion intensity. To eliminate noise, signals with the same *m/z* appearing in at least two sequential spectra were selected.

Adjustment of LC Time Jitter

To rectify the change in RT a compensatory function was calculated to maximize the correlation coefficient (CC) between the reference (A) and target (B) data (Fig. 1*A*). To increase the calculation speed and to provide robustness, the maximal value of every 1 *m/z* in each RT was substituted for the ionic strength of peaks. A dynamic programming algorithm (18, 24) was used to find the path that would yield the optimal correspondence position by using two-dimensional lattice coordinates at each cycle number (ascending RT order) of A and B. We defined coordinate values as L, gap penalty as g, CC between the mass spectra in n and m cycles of A and B as $R(A(n), B(m))$, and the total number of cycles of A and B as N and M, respectively (Fig. 1*B*).

$$L(i,j) = \max \begin{cases} L(i-1,j) + g \\ L(i,j-1) + g \\ L(i-1,j-1) + R(A(i), B(j)) \end{cases} \qquad \text{(Eq. 4)}$$

(where $i = 1,\ldots, N, j = 1,\ldots, M$)

Then we selected a coordinate giving the maximal L value from the edge of the lattice and traced backward to the previous coordinate giving the maximal L value (Fig. 1*C*). The compensatory function was the curved line obtained by spline interpolation (Fig. 1*D*).

Normalization of Total Ion Intensity

To make total ion intensity equal in different sets of data, peak intensity was normalized by multiplying it by the following normalizing coefficient,

$$V_i = \frac{\bar{I}}{I_i} \qquad \text{(Eq. 5)}$$

where V_i is normalizing coefficient, I_i is the total ion intensity indicated by the i number, and $\bar{I}$ is the average ion intensity. The normalization value in this study was set between 0.8 and 1.2.

[1] The abbreviations used are: 2DICAL, two-dimensional image-converted analysis of liquid chromatography and mass spectrometry; RT, retention time; CV, coefficient of variance; CC, correlation coefficient; ACTN4, actinin-4; BCSG1, breast cancer-specific gene-1; Dox, doxycycline.

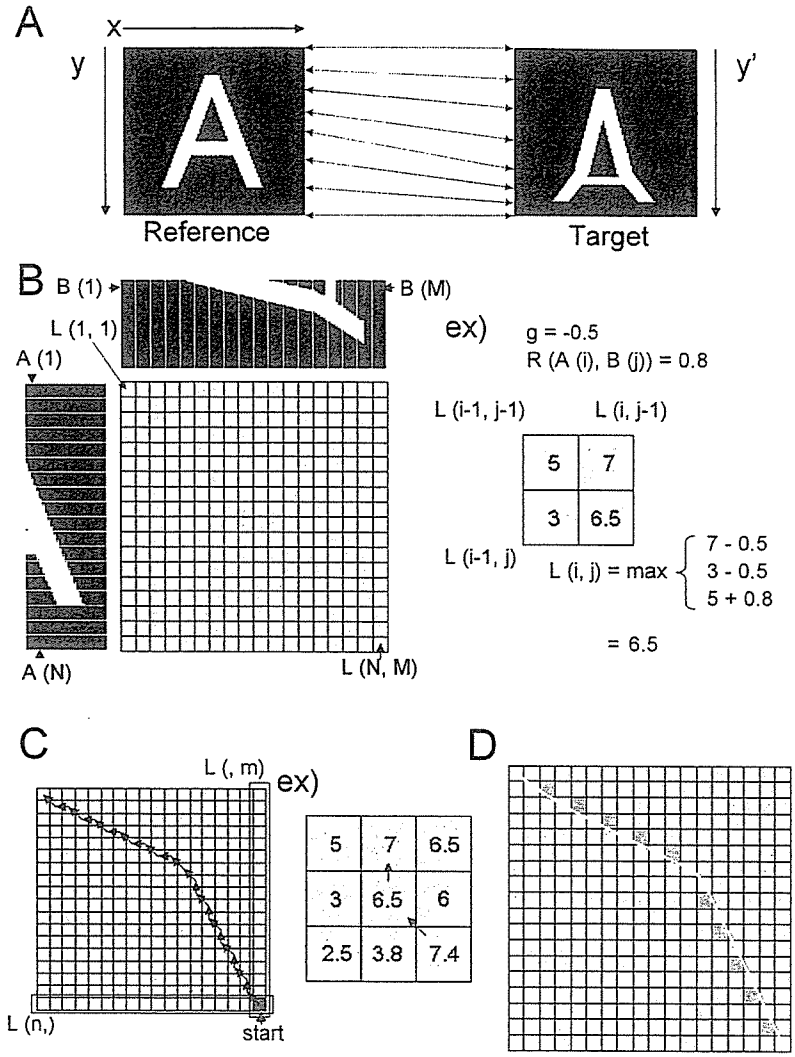

FIG. 1. **Adjustment of LC time jitter with a dynamic algorithm.** *A*, concept underlying compensation of RT changes along the *y axis*. This algorithm finds a function that compensates for time jitter y' by calculating $y = f(y')$ from target to reference. *B*, dynamic algorithm. The function is the path giving the optimal correspondence position (*yellow box* in two-dimensional lattice coordinates) in each cycle number (ascending RT order) of *A* and *B*. When the gap penalty is 0.5, the coefficient for the correlation between the mass spectra in the *i* cycle and the *j* cycle is 0.8, and the coordinate values are $L(i-1, j-1) = 5$, $L(i-1, j) = 3$, and $L(i, j-1) = 7$; then $L(i, j)$ becomes 6.5. The coordinate values of *L* in all lattices are calculated in this manner. *C*, optimal correspondence position. The optimal correspondence position starts at the lattice coordinates (k, l) where

$$(k, l) = \arg\max L(i, j) \text{ subject to: } \begin{cases} i = N, j = 1, \ldots, M \\ i = 1, \ldots, N, j = M \end{cases} \quad \text{(Eq. 6)}$$

When (k, l) is defined as V_0, the lattice coordinate is traced back. Thus

$$V_i = \arg\max L(V_{prev}), V_{prev} \in \begin{cases} V_{i-1} - (1,1) \\ V_{i-1} - (0,1) \\ V_{i-1} - (1,0) \end{cases} \quad \text{(Eq. 7)}$$

As shown in the example (*ex*), the next box to be selected has the maximum value among the *upper side*, *left side*, and *left upper side* of the former box. *D*, spline interpolation. To give the natural curve for the optimal correspondence coordinates, the coordinates arrangement of V', which gives $V_{i+1} = V_i + (1, 1)$, is extracted (the combination in the *yellow boxes*). The function is the spline interpolation to the arrangement of V'.

Peak Matching and Protein Identification

Peaks in different LC-MS runs were matched with a tolerance of ±0.25 *m/z* and ±0.5 min after alignment of the RT. Matching was confirmed by visual inspection of enlarged two-dimensional views.

MS/MS was performed on peaks having an RT and *m/z* within that range in the preparatory LC run for protein identification. Peptide fragmentation data were analyzed with Mascot software (Matrix Sciences, London, UK).

Immunoblot Analysis

Cell lysates were separated by SDS-PAGE and electroblotted onto polyvinylidene difluoride membranes (Millipore). Anti-hemagglutinin monoclonal antibody was purchased from Roche Applied Science, anti-breast cancer-specific gene-1 (BCSG1) goat polyclonal antibody (C-20) was from Santa Cruz Biotechnology (Santa Cruz, CA), anti-cytokeratin 18 (RCK16) and anti-cytokeratin 19 (BA17) monoclonal antibodies were from Chemicon (Temecula, CA), and anti-β-actin monoclonal antibody (AAN02) was from Cytoskeleton (Denver, CO). The membranes were incubated with horseradish peroxidase-conjugated secondary antibodies and visualized with an enhanced chemiluminescence kit (Amersham Biosciences) (25).

RESULTS

Strategy for Quantitative Proteomics Using 2DICAL—To improve the reproducibility of LC without reducing its separation capacity we developed the nanoflow HPLC system utilizing a splitless direct gradient pump. Concentration of protein samples into small volumes and separation by a low flow rate HPLC with small sized reversed-phase columns significantly increase the sensitivity of ESI-MS (6, 26). In our HPLC system the dead volume was minimized, and the flow rate was reduced to the 50–200 nl/min range, but the elution gradient did not fluctuate significantly during runs of over 3 h (data not shown). Multidimensional LC does not always separate peptides in the same manner among experiments. The complexity of protein samples can be sufficiently reduced by such long runs even by one-dimensional LC separation.

We also eliminated MS/MS and tried to detect all the peptides present in a given sample by high speed survey scanning as frequently as every 1 s. MS/MS scanning is a time-consuming procedure and often overlooks minor protein fragments (10). The automatic selection of precursor ions for MS/MS is not always constant, and such uncontrolled selection is likely to reduce the reproducibility.

Three thousand six hundred mass spectrum data (Fig. 2*A*) were obtained from a 1-h LC-MS run and converted into a single two-dimensional image with *m/z* values along the *x* axis and RT along the *y* axis (Fig. 2*B*). Fig. 2*C* shows a flowchart of the experimental procedures and subsequent data processing (Fig. 2, *D–I*). Signals with the same *m/z* appearing in at least two sequential RTs were grouped and considered as a peak (described under "Experimental Procedures") (Fig. 2, *F* and *G*). After normalizing to the total ion intensity of all of the peaks, the intensity of each peak was converted to a log value and expressed as a digital spot image (Fig. 2, *H* and *I*). We were able to detect 68,243 independent peaks (spots) in a 60-μg lysate of DLD1 Tet-Off ACTN4 cells cultured in the presence of doxycycline (Dox) (19).

Detection of Actinin-4 as a Differentially Expressed Protein in the Entire Proteome of DLD1 Tet-Off ACTN-4 Cells Cultured in the Absence of Dox—We previously established a colorectal cancer cell line that is capable of inducing an actin-binding protein, actinin-4, under the strict control of the tetracycline-regulatory system (designated DLD1 Tet-Off ACTN-4) (19). Upon removal of Dox from the culture medium, DLD1 Tet-Off ACTN-4 cells showed expression of actinin-4 (Fig. 3*A*), extended filopodia, and increased their motility (19). In a model experiment we investigated whether 2DICAL could pinpoint actinin-4 as a differentially expressed protein among the entire protein content of DLD1 Tet-Off ACTN-4 cells. Whole-cell lysates of DLD1 Tet-Off ACTN-4 cultured in the presence and absence of Dox were analyzed by 2DICAL in duplicate. We noted LC time jitter among the four runs (Fig. 3*B*) with a maximum difference in RT of 296 s and an average RT difference among the four runs of 36.0 s (Fig. 3, *B* and *C*). However, it was possible to adjust the LC time jitter with the newly developed software based on the dynamic programming algorithm (Figs. 1 and 3*D*), which had been developed to search sequences for regions of similarity and to align large DNA sequences (18). Because the *m/z* value (*x* axis) of each peak did not fluctuate among runs because of the high mass accuracy and constancy of Q-TOF MS, only adjustment of RT (*y* axis) was necessary.

After the RT adjustment, the average coefficient of variance (CV) of peak intensities between duplicates reached 0.37 (Dox (+)) (Fig. 3*E*) and 0.37 (Dox (−)), and the dynamic range of peak intensity calculated by our system exceeded 10^3 (Fig. 3*E*). There were 106 peaks that were more than 10-fold more highly expressed in DLD1 Tet-Off ACTN4 cells in the absence of Dox and 68 peaks that were more than 10-fold more highly expressed in the presence of Dox (Fig. 3*F*). We further confirmed the differential expression by visual inspection (Fig. 3*F*) and by repeating the same LC-MS experiment several times (data not shown). MS/MS analysis identified 15 (Fig. 3*G*) of the 106 peaks as having been derived from actinin-4. The biological significance of the other proteins whose expression was affected by induction of actinin-4 will be described elsewhere.

Detection of Differentially Expressed Proteins in Poorly Motile Capan-1 and Highly Motile BxPC3 Pancreatic Cancer Cells—Finally we compared the protein expression profiles of two pancreatic cancer cell lines, Capan-1 and BxPC3 (20), to determine whether 2DICAL is applicable to comparisons of proteomes with large differences because most of the protein (Fig. 3) as well as mRNA (data not shown) content of DLD1 Tet-Off ACTN-4 cells was unchanged after removing Dox, and that may have simplified the adjustment of the sample-to-sample time jitter. We noted that a significant number of spots were detected equally in Capan-1 cells and BxPC3 cells (Fig. 4*A*, *yellow spots*), making it possible to perform time adjustment of similar quality to that for DLD1 Tet-Off ACTN4 cells. In addition, a total of 15,407 spots that were differentially expressed between Capan-1 and BxPC3 were detected (9692 spots that were expressed more abundantly in Capan-1 than in BxPC3 and 5715 spots that were expressed more abundantly in BxPC3 than in Capan-1, $p < 0.01$, Student's *t* test, between triplicates) (Fig. 4*B*, *red* and *green spots*) after subtracting spots that were equally expressed by both (Fig. 4*A*, *yellow spots*). A representative differentially expressed pep-

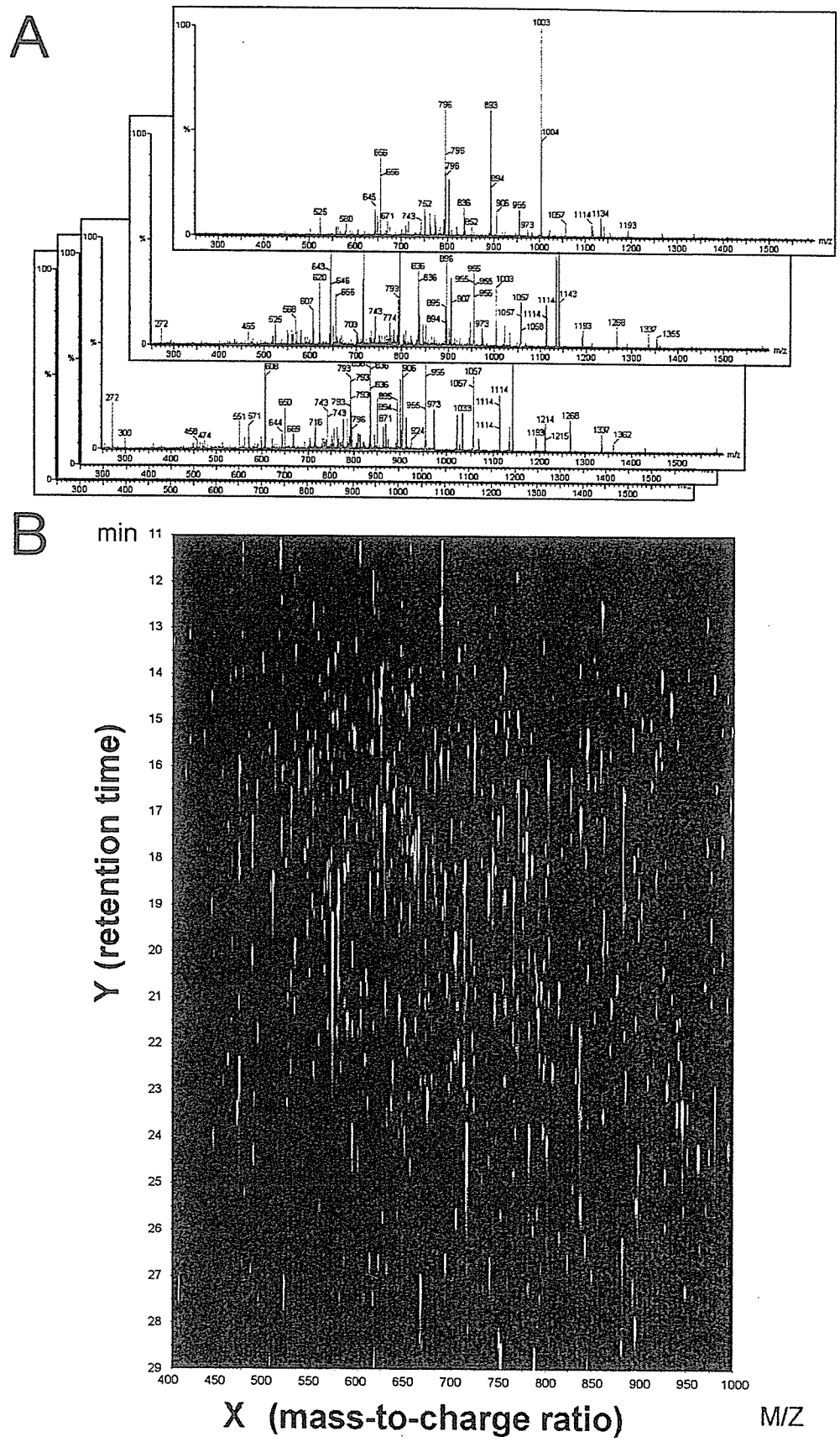
A
B
min
Y (retention time)
X (mass-to-charge ratio)
M/Z

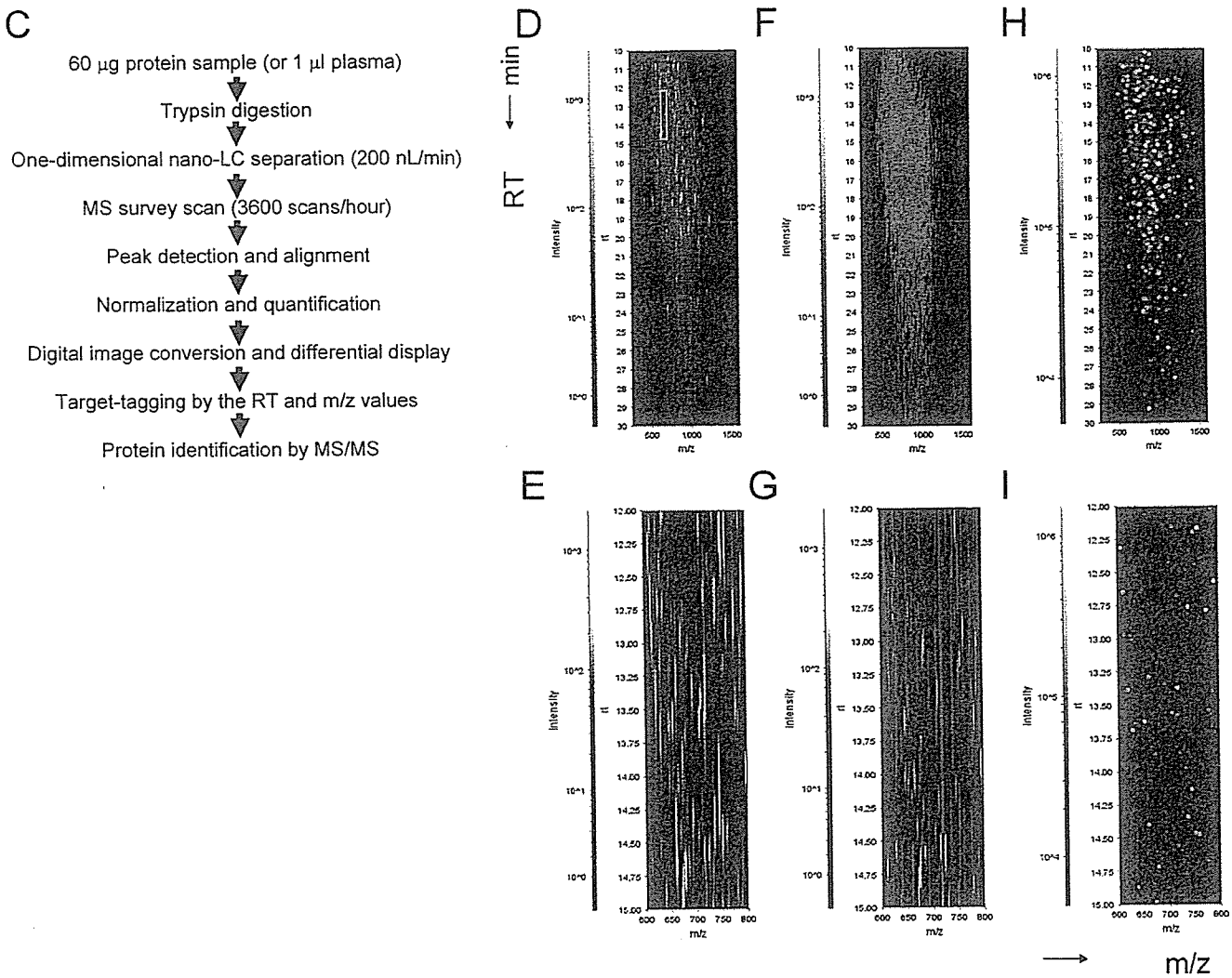

FIG. 2—*continued*

tide is shown in Fig. 4*C* (*red arrow*). Peaks were tagged by their intrinsic RT and *m/z* values, and MS/MS was performed on peaks having the same RT and *m/z* in the preparatory LC run for protein identification (Fig. 2*C*). Protein identification and differential expression were confirmed by immunoblotting with available antibodies. Fig. 4*D* shows representative data: BCSG1 (27), cytokeratin 19, and cytokeratin 18 were expressed more abundantly in the poorly motile Capan-1 cells than in the highly motile pancreatic cancer BxPC3 cells.

DISCUSSION

We reviewed various aspects of LC-MS for application to large scale quantitative proteomics and eliminated factors that reduce reproducibility and/or comprehensiveness, such

FIG. 2. **Strategy for quantitative proteomics using 2DICAL.** *A*, raw LC-MS mass spectra obtained from 1 μl of plasma from a healthy volunteer. A 1-h LC-MS run yielded 3600 mass spectra, which were used for two-dimensional image analysis. *B*, two-dimensional display of a plasma peptide array with the *m/z* values (400–1,000 *m/z*) along the *horizontal* (*x*) *axis* and RT (11–29 min) along the *vertical* (*y*) *axis*. *C*, flowchart for experimental procedures and data processing. *D*, two-dimensional raw image of the proteome of DLD1 Tet-Off ACTN4 cells with *m/z* values (250–1,600 *m/z*) along the *x axis* and RT (10–30 min) along the *y axis*. *E*, enlargement of the *light blue square* area in *D*. *F* and *G*, peak detection. The peaks appearing in *D* and *E* were picked up by using the algorithm described under "Experimental Procedures," and these are shown in the *red squares*. In *G* only peaks having intensity greater than 50,000 are *highlighted*. Peak intensity is the sum of the intensities of grouped signals. *H* and *I*, digital image conversion of the peaks detected in *F* and *G*. The virtual spots are located at *m/z* as monoisotopic molecular weights and at RT as the gravity center of ion intensity. The *brightness* of the spots corresponds to the peak intensity, defined as the integral of ion intensity of grouped signals, as described under "Experimental Procedures." As a result, the spot intensity exceeds 10^3, although the Q-TOF detector is saturated at thousands of counts per second (14, 16). The areas of *F* and *H* corresponding to the area in the *light blue square* in *D* have been enlarged, and these are shown in *G* and *I*, respectively.

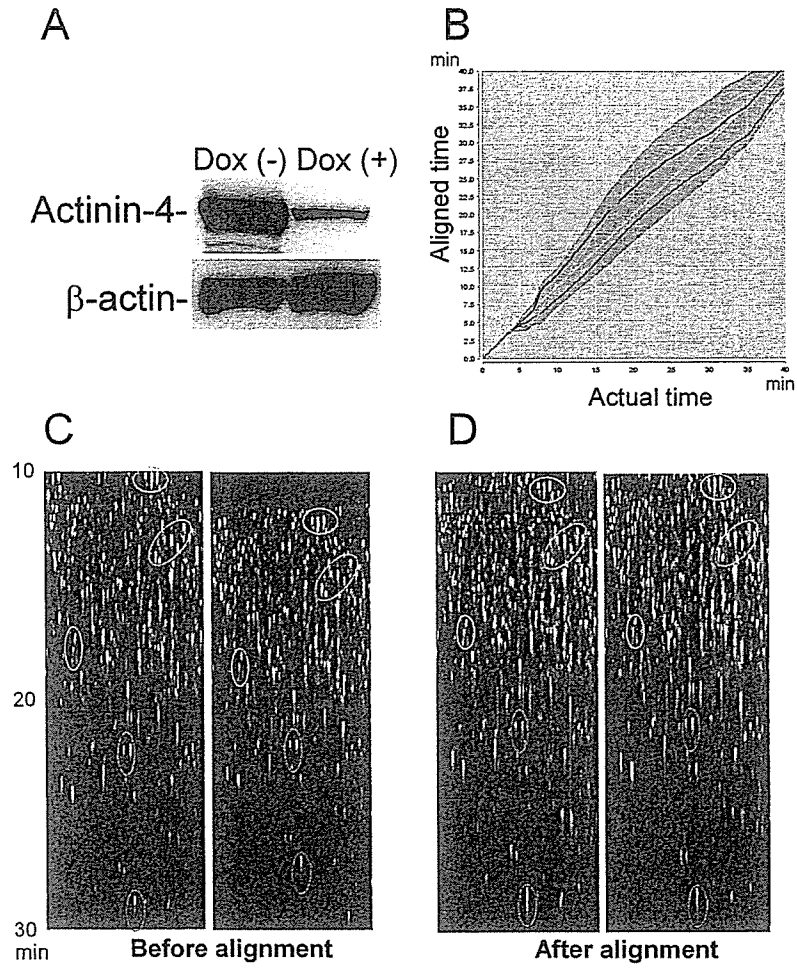

FIG. 3. **Detection of actinin-4 as a differentially expressed protein in the entire proteome of DLD1 Tet-Off ACTN-4 cells cultured in the absence of Dox.** *A*, immunoblot analysis of DLD1 Tet-Off ACTN4 cells cultured in the presence (+) and absence (−) of 0.1 μg/ml Dox for 72 h with anti-hemagglutinin antibody (to detect induced actinin-4) and anti-β-actin antibody (internal control). *B*, RT calibration curves of four 40-min LC runs. Lysates of DLD1 Tet-Off ACTN4 cells cultured in the presence (*blue* and *red lines*) and absence (*green* and *light blue lines*) of Dox were analyzed in duplicate (total, four runs). The *horizontal* (*x*) *axis* represents actual RT, and the *vertical* (*y*) *axis* represents adjusted RT. The average and maximum RT differences from a reference run of DLD1 Tet-Off ACTN4 cells cultured in the presence of Dox (*straight blue line* with a *slope* of 45°) of the three other runs were 36.0 and 296 s, respectively. *C*, 2DICAL images of duplicate runs of DLD1 Tet-Off ACTN4 cultured in the presence of Dox before the RT alignment. Representative peaks are highlighted in *light blue*, *yellow*, *green*, *pink*, and *red circles*. *D*, 2DICAL images of duplicate runs of DLD1 Tet-Off ACTN4 cells cultured in the presence of Dox after the RT alignment. Representative peaks are highlighted in *light blue*, *yellow*, *green*, *pink*, and *red circles*. *E*, reproducibility between duplicate runs of DLD1 Tet-Off ACTN4 cells cultured in the presence of Dox after the RT alignment. The *horizontal* (*x*) *axis* represents the distribution of peak intensities of the first run, and the *vertical* (*y*) *axis* represents that of the second run. The intensity CC between the two runs is 0.97. The average CV of all 68,243 peaks was 0.37. The average CV for DLD1 Tet-On ACTN4 cells cultured in the absence of Dox was 0.37 (data not shown). More than 70% of the duplicate peaks were plotted within a 2-fold difference (*blue lines*), and more than 90% were plotted within a 3-fold difference (*red lines*). We are able to detect 6.3-fold changes with 95% confidence. *F*, a representative peptide differentially expressed in DLD1 Tet-Off ACTN4 cells after removal of Dox and appearing at 717.4 *m/z* and 13.30 min. *G*, 15 peptide fragments appearing in DLD1 Tet-Off ACTN4 cells after removal of Dox and identified as derived from actinin-4 by MS/MS analysis. The *m/z* values, RT, and amino acid sequences of these 15 peptides are shown at the *right*.

as sample labeling, multidimensional LC separation, and MS/MS (Fig. 2*C*). However, the key technology of our platform is the application of the dynamic algorithm developed to align large DNA sequence data to the alignment of large peptide peak data generated by nano-LC-MS. Aebersold and colleagues (10, 28) also claimed that RT alignment is necessary to compare different LC-MS data and reported a new software suite. They first reduced the complexity of serum/plasma samples by extracting *N*-glycoproteins and identified 1000–5000 peaks from one set of LC-MS data. They reported a mean CV of 0.31 over four runs, and ~12% of the peptides were missed by the procedure (10). Wang *et al.* (14) detected ~3400 molecular ions in 25 human serum samples with a median CV of 25.7%. Our alignment method is capable of analyzing a much larger number of peaks with reasonable computing speed (2 h for the comparative analysis of two

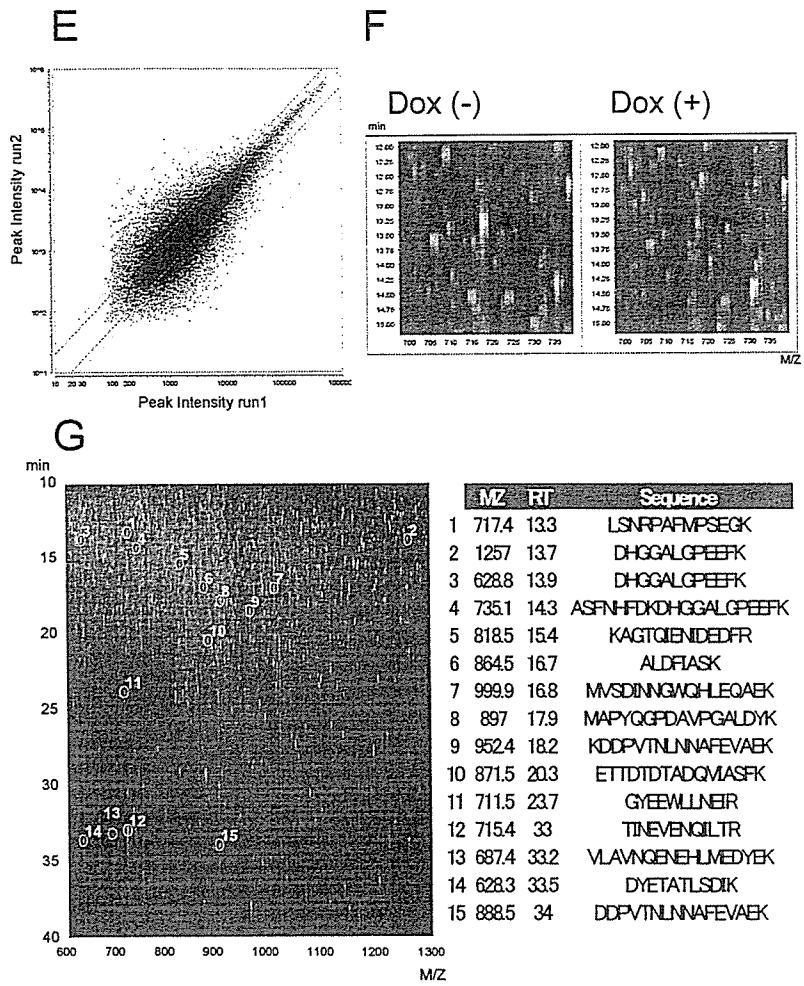

FIG. 3—*continued*

LC-MS experiments). We were able to detect more than 100,000 peaks in unlabeled and unfractionated protein samples and obtained equivalent but slightly higher CV values (0.35–0.39) than in their studies (Fig. 3*E*). We confirmed the efficacy of 2DICAL for quantitative protein analysis using two model experiments: an experiment that compared proteomes with small differences (Fig. 3) and another that compared proteomes with large differences (Fig. 4).

Bogdanov and Smith (29) reported two-dimensional display of capillary LC-FTICR analysis in which it was possible to detect more than 100,000 peaks and 1000 proteins in a single run and yielded a dynamic range of peak intensities of 10^3. We were able to obtain a comparable level of comprehensiveness using an easy-to-use and common MS instrument. Our alignment software seems ideal for comparative analysis of large data sets generated by LC-FTICR-MS. However, reduction of sample complexity in both platforms still seems necessary for detection of low abundance serum or plasma proteins because the concentration ranges of serum/plasma proteins span an estimated >10 orders of magnitude (30). Furthermore decreased sample complexity significantly reduces computing time and improves the accuracy of peak matching.

We consider the development of 2DICAL to still be in the early stage. Its reliability in regard to matching and quantification of low intensity peaks is not expected to be as high as for high intensity peaks. Because mismatching of peaks has a significant adverse effect on quantification, deliberate effort must be made to eliminate mismatching by visual inspection (Figs. 3*F* and 4*C*) and by recalculation. Differential protein expression cannot be identified based on statistical data alone. At a p value of <0.01, one would expect 1% of measured values to appear regulated due to variance in the data alone. Confirmatory reruns of different lots of samples were always necessary before targeted LC-MS/MS. Protein identification and differential expression also need to be confirmed by Western blotting whenever antibodies are available (Fig. 4*D*). We are now accumulating 2DICAL data to construct a two-dimensional map linking the m/z and RT of peptides to their amino acid sequences.

The amount of data obtained in one LC-MS experiment reached 2 gigabytes. The optimal number of samples for comparing seems to be determined by computer capacity.